Journal of Solid State Chemistry 182 (2009) 995–1002

Contents lists available at ScienceDirect

Journal of Solid State Chemistry

journal homepage: www.elsevier.com/locate/jssc

Ti_2GaC, Ti_4GaC_3 and Cr_2GaC—Synthesis, crystal growth and structure analysis of Ga-containing MAX-phases $M_{n+1}GaC_n$ with M = Ti, Cr and n = 1, 3

Johannes Etzkorn [a,b], Martin Ade [a,b], Dominik Kotzott [a,b], Monique Kleczek [c,1], Harald Hillebrecht [a,b,*]

[a] Institut für Anorganische und Analytische Chemie, Albert-Ludwigs-Universität Freiburg, Albertstrasse 21, D-79104 Freiburg, Germany
[b] Freiburger Materialforschungszentrum FMF, Stefan-Maier-Strasse 25, D-79104 Freiburg, Germany
[c] University of Toronto, Canada

ARTICLE INFO

Article history:
Received 11 November 2008
Received in revised form
27 December 2008
Accepted 3 January 2009
Available online 13 January 2009

Keywords:
Single crystal growth
Crystal structure
Energy dispersive X-ray spectroscopy (EDXS)
X-ray diffraction (XRD)
Carbides

ABSTRACT

Single crystals of Ga-containing MAX-phases Ti_2GaC, Ti_4GaC_3, and Cr_2GaC were grown from a metallic melt generated by an excess of Ga. This technique allows the crystal growth at different temperatures to control the product distribution. Compounds developed were Ti_2GaC and TiC at 1500 °C, and Ti_2GaC and Ti_4GaC_3 at 1300 °C. Crystal structures were refined from single crystal data. Ti_2GaC and Cr_2GaC were previously known, and belong to the Cr_2AlC type as well as the solid solutions $V_2Ga_{1-x}Al_xC$ and $Cr_2Ga_{1-x}Al_xC$. Ti_4GaC_3 is one of the few 413-phases ($P6_3/mmc$, $a = 3.0690(4)$ Å, $c = 23.440(5)$ Å) and the first Ga-containing representative. The crystal structures of MAX-phases are intergrowths of layers of an intermetallic MGa in a hexagonal stacking sequence with carbidic layers $(MC)_n$ of the NaCl type. The thickness of the layer depends from the value of n. The results of the structure refinements also demonstrate that also the structural details follow this description.

1. Introduction

Binary carbides and nitrides of group IV and V transition metals are important high temperature hard materials with extremely high melting points [1]. Recent investigations on ternaries such as Ti_3SiC_2 [2], Ti_3AlC_2 [3], Ti_4AlN_3 [4] and related compounds of the series $(MX)_n(MA)$ (M = "early" transition metal; A = main group metal; X = C, N; n = 1,2,3,… [5] ("MAX-phases") have shown excellent and unique material properties like damage and shock resistance or good thermal and electrical conductivity [6]. Among them compounds with the composition $M_2M'X$ (H-phase or 211-phase) are the most numerous by far. While M is usually a group 4 or 5 transition metal A shows high variability. It can be a main group metal (Al, Ga, In, Tl, Sn, Pb) or a meta–metal (Si, Ge, P, As) [6,7]. Most of the H-phases were already synthesised and characterised in the 1960s by Nowotny, Jeitschko, and coworkers [8,9].

According to their unique material properties [10] recent investigations focused on MAX-phases with A = Al and Si. Furthermore higher MAX-phases, i.e. 312- and 413-phases (n = 2, 3) are only known for A = Al, Si and Ge. Single crystal growth, especially of the higher MAX-phases, is difficult because of the high melting points. Therefore, studies of single crystals are very rare and most of the investigations deal with powder samples. Recently we have reported on synthesis and single crystal growth of the 413-phases Ta_4AlC_3 [11], and V_4AlC_{3-x} [12] using metal flux techniques. Furthermore we were able to prove the existence of solid solutions ($Ti_4Al_{1-y}Sn_yN_{3-x}C_x$ [13]), carbon vacancies (V_4AlC_{3-x}, $x \approx 0.31$) [12]) and ordered super structures $V_{12}Al_3C_8$ [12]). In this article, we will report on the H-phases M_2GaC (M = Ti, Cr), the solid solutions $V_2Ga_{0.4}Al_{0.6}C$ and $Cr_2Ga_{0.4}Al_{0.6}C$, and Ti_4GaC_3, the first Ga-containing higher MAX-phase.

2. Experimental section

2.1. Syntheses, crystal growth, and characterisation

Single crystals of Ti_2GaC, Cr_2GaC, Ti_4GaC_3 and the solid solution $V_2Ga_{1-x}Al_xC$ were synthesised from the elements with an excess of gallium. $Cr_2Ga_{0.4}Al_{0.6}C$ was found as a by-product in the system Ga/Cr/C. As shown in Fig. 1, the distribution of products is significantly dependant on the temperature of the synthesis. Accordingly, the conditions were selected.

EDX (energy dispersive X-ray spectroscopy) and WDX (wavelength dispersive X-ray spectroscopy) measurements were performed on single crystals to ensure the correct composition. The ratio of M:Ga was determined by EDX with an accuracy of

* Corresponding author. Fax: +49 761 203 6102.
E-mail address: harald.hillebrecht@ac.uni-freiburg.de (H. Hillebrecht).
[1] On leave from University of Toronto, Canada.

0022-4596/$ - see front matter © 2009 Elsevier Inc. All rights reserved.
doi:10.1016/j.jssc.2009.01.003

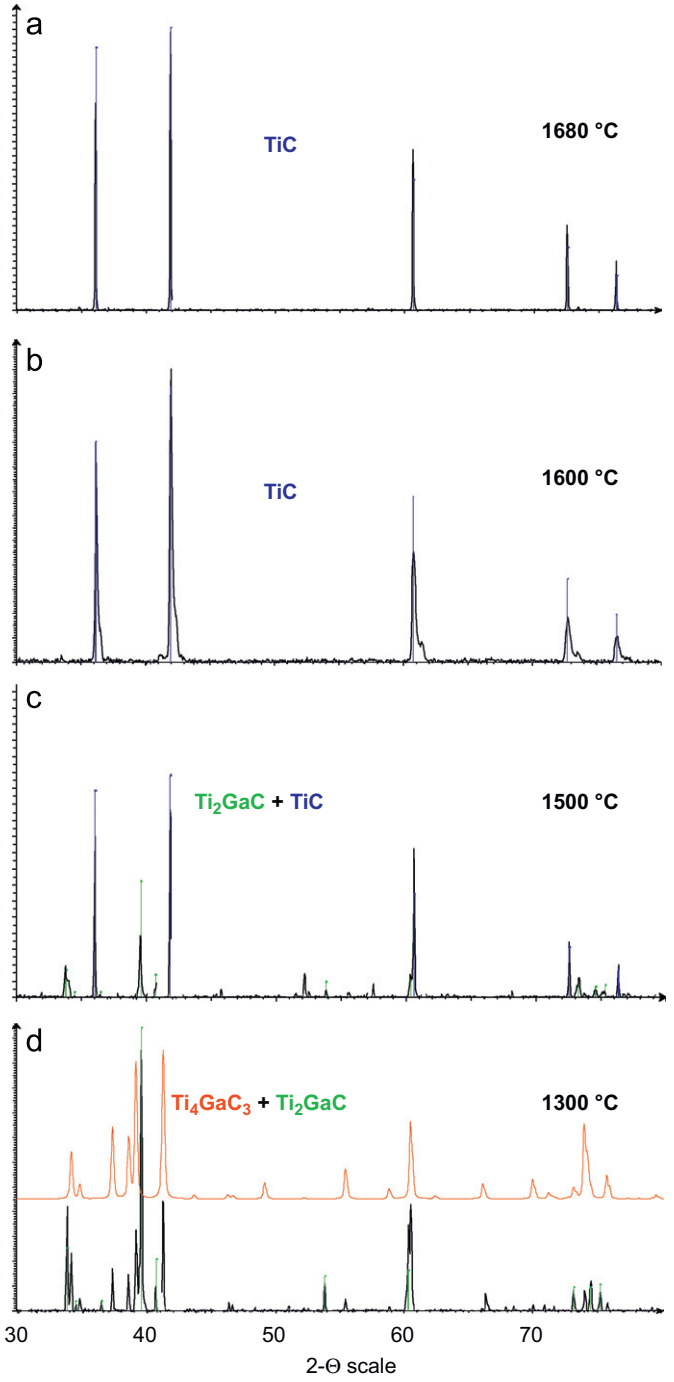

Fig. 1. Powder patterns from Ti/Ga/C; synthesis at: (a) 1680 °C, (b) 1600 °C, (c) 1500 °C, and (d) 1300 °C, calculated pattern for Ti_4GaC_3 (upper part in d)) is simulated from single crystal data.

±1 mol%. Furthermore WDX measurements were necessary to exclude the incorporation of light elements with Z between 4 and 13 because Ti frequently contains small amounts of nitrogen caused by the high stability of TiN. Especially nitrogen is able to substitute carbon in binary and ternary M carbides [1] and cannot be reliably determined from X-ray data. WDX will detect nitrogen in amounts exceeding 3 mol%. Accuracy for the WDX was poorer comparable to the EDX in the simultaneous determination of C and other metals due likely to scaling problems [14,15].

XRD patterns were recorded with a Siemens D5000 (Cu$K\alpha$1 radiation, Ge-monochromator, gas-filled PSD, Debye–Scherrer geometry, transmission). Single crystal investigations were done at room temperature using graphite monochromated Mo$K\alpha$ radiation. A numerical absorption correction was applied using equivalent method (Programme XSHAPE/XRED [18]). Structure models for the refinements (programme SHELXTL [19]) were taken from the literature.

SEM pictures and EDX measurements were performed using a Jeol SM 6400 (Ge detector). For WDX investigations, we employed the Cameca SX 50 (analyzer crystal PC2, diamond and c-BN as standards).

Ti_2GaC: Single crystals of Ti_2GaC were obtained from the elements by the following procedure. Commercially available powders (Ti, Ventron, 99.5%; C, graphite, Chempur, 99.9+%), or small pieces (Ga, Alfa Aesar, 99.99%) were mixed in a ratio of 5:2:7 and pressed into a pellet (total mass: ca. 300 mg). The pellet was put into a corundum crucible and quickly (200 K/h) heated to 1500 °C under an argon atmosphere. The sample was held for 50 h at 1500 °C, cooled to 900 °C with a cooling rate of 5 K/h, held for 30 h and then cooled at 30 K/h to 600 °C and with 100 K/h to RT. The excess metal of the solidified melt was removed by dissolving the regulus in half-concentrated aqueous HCl. The residue was washed and dried. Small hexagonal platelets were identified as Ti_2GaC. The XRD pattern was indexed with a hexagonal unit cell with $a = 3.0663(4)$ Å and $c = 13.312(2)$ Å (Fig. 1c). Additional lines were assigned to TiC or Ti_4GaC_3. EDX measurements on selected single crystals revealed a ratio Ti:Ga of 69:31. WDX investigations confirmed the presence of the elements Ti, Ga and C and the absence of N and O.

Ti_4GaC_3: Single crystals of Ti_4GaC_3 were obtained from the elements similar to Ti_2GaC, but at lower temperatures. Ti, C, and Ga were mixed at a ratio of 5:2:10 (total mass 300 mg) and pressed to a pellet. The temperature program was the same as for Ti_2GaC, but 1300 °C as the maximum temperature. After dissolution the residue contained hexagonal platelets (Ti_2GaC) and columns (Ti_4GaC_3, Fig. 2). The powder pattern showed the lines of Ti_2GaC and Ti_4GaC_3 (Fig. 1d). The refinement of the indexed reflections resulted in a hexagonal unit cell with $a = 3.0582(8)$ Å and $c = 23.370(4)$ Å. EDX measurements on selected single crystals revealed a ratio of 80:20 for Ti:Ga and the absence of other elements with $Z > 13$. WDX investigations confirmed the presence of the elements Ti, Ga, and C, an atomic ratio of 47:11:42 and the absence of N and O.

Cr_2GaC: Single crystals of Cr_2GaC were obtained from the elements. Commercially available powders (Cr, Alfa Aesar, 99.5%; C, graphite, Chempur, 99.9+%) or small pieces (Ga, Alfa Aesar,

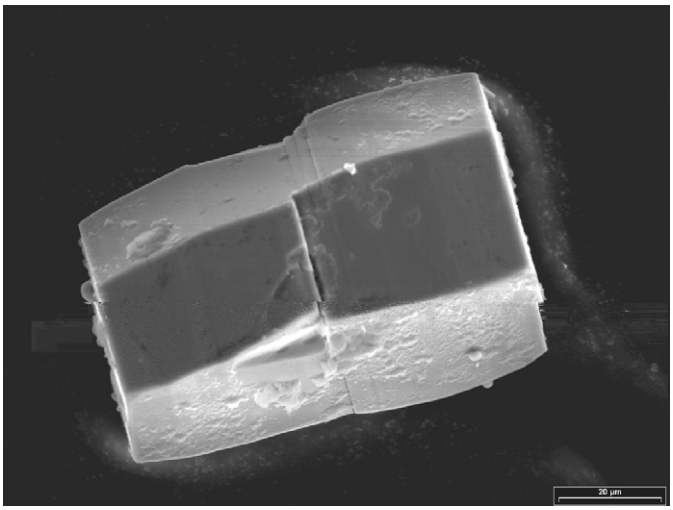

Fig. 2. SEM picture of a Ti_4GaC_3 single crystal.

99.99%) were mixed at a ratio of 5:2:11, pressed into a pellet (total mass: ca. 300 mg) and submitted to the same procedure as described for the Ti compounds ($T_{max} = 1300\,°C$). Small hexagonal platelets were characterised as Cr_2GaC. The XRD pattern was indexed with a hexagonal unit cell with $a = 2.8929(8)$ Å and $c = 12.648(4)$ Å. EDX measurements on selected single crystals revealed a ratio Cr:Ga of 66:34.

$V_2Ga_{1-x}Al_xC$: Small single crystals were obtained from the elements. Commercially available powders (V, ChemPur, 99.5+%; Al, 99.9%, Ventron; C, Carbon Black, Strem Chemicals, 99.9+%) or small pieces (Ga, Alfa Aesar, 99.99%) were mixed at ratios of 6:10:1:5 and 6:7.5:1:7.5, pressed into a pellet (total mass: ca. 300 mg) and submitted to the same procedure like the Ti-compounds ($T_{max} = 1500\,°C$). Very small hexagonal platelets were characterised as 211-phases. Small amounts of V_6C_5 [7] were found as a by-product. The XRD pattern of the Al-rich sample was indexed with a hexagonal unit cell with $a = 2.921(1)$ Å and $c = 13.047(9)$ Å. The values for the sample with equal amounts of Al and Ga were $a = 2.928(1)$ Å and $c = 12.998(5)$ Å. EDX measurements on selected single crystals revealed a ratio Cr:Ga:Al of 65:16:19 and 66:20:14, respectively.

$Cr_2Ga_{1-x}Al_xC$ ($x \approx 0.60$): A few small black hexagonal platelets were obtained, with single crystals of Cr_7C_3 [16] as a by-product, from the reaction of Cr, Ga, and C (molar ratio 5:7:2) at 1680 °C in a corundum crucible. X-ray investigations revealed a 211-MAX-phase. The XRD pattern was indexed with a hexagonal unit cell with $a = 2.8668(13)$ Å and $c = 12.762(6)$ Å. In agreement with the EDX results the refinement of the single crystal data resulted in a mixed crystal $Cr_2Ga_{1-x}Al_x$ with $x \approx 0.60$). This composition was confirmed for several crystals of this batch. The unexpected Al content may be explained by the high reaction temperature in combination with the Al_2O_3 crucible.

2.2. Structure solution and refinement

Ti_2GaC: A black hexagonal platelet was isolated from the Ga-melt and investigated using a single crystal diffractometer equipped with an image plate detector (STOE, IPDS I, MoKα radiation). All reflections were indexed with a hexagonal unit cell with lattice parameters of $a = 3.0764(4)$ Å and $c = 13.378(3)$ Å. Unit cell dimensions and reflection conditions (hhl with $l = 2n$) were characteristic for a H-phase. The refinement was started with the parameters of a Cr_2AlC type [8] in space group $P6_3/mmc$ and performed quick convergence. Finally R-factors of $R_1(F) = 0.0267$ and $wR_2(F^2) = 0.0628$ were obtained with 103 unique reflections (61 with $I > 2\sigma(I)$) and 10 parameters. Details are listed in Tables 1–3.

Ti_4GaC_3: A hexagonal column was isolated from the Ga melt which had been heated to1300 °C. According to unit cell dimensions ($a = 3.0690(4)$ Å, $c = 23.440(5)$ Å), symmetry (Laue-class $6/mmm$), and reflection conditions (hhl with $l = 2n$) the refinement was started in space group $P6_3/mmc$ with the structure model of a 413-phase [11–13]. At the final stage of the refinement, it was discovered that the displacement parameter of Ga on site 2c was much too large (factor of 3) compared to Ti_2GaC. Furthermore an additional site (2d) occurred with a residual density of 5.7 $e^-/Å^3$. According to the crystal structure and the results of the elemental analysis (see below) two partially occupied positions for Ga were introduced. A refinement with free occupation factors yielded values of 81.6(13)% for site 2c and of 8.9(8)% for site 2d ($R_1(F) = 0.040$, $wR_2(F^2) = 0.103$). The assumption of a complete occupation of the Ga-layer (sof's of 2d and 2c sum up to 1/12) resulted in occupations of 86.1(14)% and 13.9(14)%. Because defects on the A-site are not described for MAX-phases and in agreement with the EDX results we utilised

Table 1
Structure refinement of Ti_2GaC, Ti_4GaC_3, Cr_2GaC, $V_2Ga_{1-x}Al_xC$ ($x = 0.56, 0.43$), and $Cr_2Ga_{0.40}Al_{0.60}C$.

	Ti_2GaC	Ti_4GaC_3	Cr_2GaC	$Cr_2Ga_{0.4}Al_{0.6}C$	$V_2Ga_{0.44}Al_{0.56}C$	$V_2Ga_{0.57}Al_{0.43}C$
Crystal shape	Hexagonal platelet	Hexagonal prism	Hexagonal platelet	Hexagonal platelet	Hexagonal platelet	Hexagonal platelet
Crystal colour	Metallic lustrous	Metallic lustrous	Metallic lustrous	Metallic lustrous	Metallic lustrous	Metallic lustrous
Crystal size (mm^3)	0.1 × 0.1 × 0.01	0.025 × 0.025 × 0.1	0.05 × 0.05 × 0.001	0.04 × 0.04 × 0.001	0.02 × 0.02 × 0.001	0.02 × 0.02 × 0.001
Formula weight (g/mol)	177.49	297.27	185.73	160.08	159.74	160.08
Crystal system	Hexagonal	Hexagonal	Hexagonal	Hexagonal	Hexagonal	Hexagonal
Space group	$P6_3/mmc$	$P6_3/mmc$	$P6_3/mmc$	$P6_3/mmc$	$P6_3/mmc$	$P6_3/mmc$
Lattice constants	$a = 3.0764$ (4) Å, $C = 13.378$ (3) Å	$a = 3.0690$ (4) Å, $b = 23.440$ (5) Å	$a = 2.9008$ (4) Å, $c = 12.632$ (3) Å	$a = 2.875$ (2) Å, $c = 12.679$ (11) Å	$a = 2.9199$ (17) Å, $c = 13.029$ (8) Å	$a = 2.9252$ (13) Å, $c = 12.959$ (9) Å
Cell volume ($Å^3$)	109.65	191.20	92.05	90.77	96.20	96.03
Formula units	2	2	2	2	2	2
Density, calculated (g/cm^3)	5.38	5.17	6.70	5.86	5.52	5.71
Radiation	MoKα	MoKα	MoKα	MoKα	MoKα	MoKα
θ-range	$-4 \leq h \leq 4$, $-4 \leq k \leq 4$, $-20 \leq l \leq 20$	$-4 \leq h \leq 4$, $-4 \leq k \leq 4$, $-30 \leq l \leq 30$	$-4 \leq h \leq 4$, $-4 \leq k \leq 4$, $-18 \leq l \leq 18$	$-4 \leq h \leq 4$, $-4 \leq k \leq 4$, $-19 \leq l \leq 19$	$-4 \leq h \leq 4$, $-4 \leq k \leq 4$, $-22 \leq l \leq 22$	$-4 \leq h \leq 4$, $-4 \leq k \leq 4$, $-22 \leq l \leq 22$
$2\theta_{max}$ (Deg)	65	65	65	65	75	75
Diffractometer	STOE IPDS I	STOE IPDS I	STOE IPDS I	STOE IPDS I	STOE IPDS II	STOE IPDS II
Data collection	$0° \leq \omega \leq 200°$; $\varphi = 0°$, $\Delta\omega = 2°$	$0° \leq \omega \leq 200°$; $\varphi = 0°$, $\Delta\omega = 2°$	$0° \leq \omega \leq 200°$; $\varphi = 0°$, $\Delta\omega = 2°$	$0° \leq \omega \leq 200°$; $\varphi = 0°$, $\Delta\omega = 2°$	$0° \leq \omega \leq 200°$; $\varphi = 0°$, $\Delta\omega = 2°$	$0° \leq \omega \leq 200°$; $\varphi = 0°$, $\Delta\omega = 2°$
Measure time (s)	180	120	360	120	600	600
Reflections measured	1574	1265	1153	1312	637	987
Independent reflections	103	103	90	88	117	113
Reflections $I > 2\sigma(I)$	61	84	63	58	75	77
Max/min transmission	0.1321; 0.0886	0.1644; 0.0936	0.1321; 0.0886	0.1109; 0.0257	0.6418; 0.3217	0.5709; 0.2884
R_{int}, R_{sigma}	0.1105, 0.0463	0.1242, 0.0590	0.1380, 0.0338	0.1293, 0.0450	0.0611, 0.0231	0.0924, 0.0189
Absorption coefficient (mm^{-1})	18.85	14.72	25.58	17.51	15.50	17.19
Extinction coefficient [19]	0.025 (9)	0.030 (14)	0.294 (19)	0.015 (15)	0.337 (42)	0.298 (29)
Residual electron $e^-/Å^3$ min, max, sigma	+0.94, −0.87, 0.23	+1.87, −3.53, 0.31	+0.48, −0.56, 0.16	+0.61, −0.74, 0.19	+0.75, −1.32, 0.22	+0.46, −0.68, 0.13
Weighting function [19]	0.0338; 0.0	0.0592; 2.71	0.028; 0.0	0.0262; 0.03	0.0421; 0.0	0.0247; 0.0
Number of parameters	9	14	9	9	10	10
R-factors	$R_1(F) = 0.0267$; $wR_2(F^2) = 0.0628$	$R_1(F) = 0.0516$; $wR_2(F^2) = 0.125$	$R_1(F) = 0.0174$; $wR_2(F^2) = 0.0461$	$R_1(F) = 0.0326$; $wR_2(F^2) = 0.0848$	$R_1(F) = 0.0278$; $wR_2(F^2) = 0.0636$	$R_1(F) = 0.0158$; $wR_2(F^2) = 0.0357$

Table 2
Coordinates, displacement parameters (in 10^4 Å^2), and site occupation factors[a].

Compound atom	Site	x	y	z	U_{eq}	sof[b]	U_{11}	U_{33}
Ti_2GaC								
Ti	4*f*	1/3	2/3	0.08653 (13)	160 (4)	1.01 (1)	57 (5)	69 (8)
Ga	2*d*	2/3	1/3	1/4	128 (6)	0.98 (1)	138 (7)	108 (9)
C	2*a*	0	0	0	74 (28)	1.04 (5)	60 (36)	102 (45)
Ti_4GaC_3								
Ti1	4*e*	0	0	0.15637 (10)	117 (8)	1.00 (2)	86 (11)	179 (14)
Ti2	4*f*	1/3	2/3	0.05582 (11)	124 (8)	1.00 (2)	83 (11)	205 (14)
Ga	2*c*	1/3	2/3	1/4	141 (10)[c]	0.86 (1)[c]	283 (19)[c]	218 (19)[c]
Ga′	2*d*	2/3	1/3	1/4	141 (10)[c]	0.14 (1)[c]	283 (19)[c]	218 (19)[c]
C1	4*f*	2/3	1/3	0.1065 (6)	178 (30)[d]	1.02 (7)		
C2	2*a*	0	0	0	13 (27)[d]	1.42 (10)		
Cr_2GaC								
Cr	4*f*	1/3	2/3	0.08527 (5)	95 (3)	1.00 (1)	88 (4)	110 (4)
Ga	2*d*	2/3	1/3	1/4	123 (4)	1.00 (1)	129 (4)	112 (5)
C	2*a*	0	0	0	111 (12)	1.05 (4)	95 (17)	145 (27)
$V_2Ga_{0.44}Al_{0.56}C$								
V	4*f*	1/3	2/3	0.08579 (5)	50 (3)	1.00 (1)	48 (4)	54 (4)
Al/Ga[c]	2*d*	2/3	1/3	1/4	82 (5)	0.559/0.441 (7)[c]	94 (6)	59 (5)
C	2*a*	0	0	0	59 (9)	1.09 (4)	44 (14)	87 (16)
$V_2Ga_{0.57}Al_{0.43}C$								
V	4*f*	1/3	2/3	0.08587 (3)	58 (2)	1.00 (1)	58 (2)	57 (3)
Al/Ga[c]	2*d*	2/3	1/3	1/4	86 (3)	0.434/0.566 (4)[c]	99 (3)	59 (3)
C	2*a*	0	0	0	67 (6)	0.99 (3)	65 (9)	71 (10)
$Cr_2Ga_{0.40}Al_{0.60}C$								
Cr	4*f*	1/3	2/3	0.08512 (7)	139 (5)	1.00 (1)	128 (6)	162 (7)
Al/Ga[c]	2*d*	2/3	1/3	1/4	168 (8)	0.599/0.401 (4)[c]	165 (9)	173 (10)
C	2*a*	0	0	0	184 (18)	1.03 (3)	–	–

[a] esd's in parentheses, $U_{11} = U_{22} = 2\ U_{12}$, $U_{23} = U_{13} = 0$.
[b] In order to check for mixed occupations and/or vacancies site occupation factors were treated by turns as free variables at the end of the refinement.
[c] Coupled refinement (see text).
[d] U_{iso}.

the idealised composition Ti_4GaC_3 for the discussion. In contrast to the refinement of Ti_2GaC, Cr_2GaC and several other MAX-phases like Ta_4AlC_3 [11], Ta_3AlC_2 [11] and V_2AlC [12] the displacement parameter of carbon on the special site 2*a* is very small and the site occupation factor is significantly enlarged. Because nitrogen and oxygen were not detected for this single crystal it is probably caused by the disorder of Ga and other defects like stacking faults which can influence the electron density at the origin and other very special sites. Therefore the carbon atoms were refined with isotropic displacement parameters. Finally *R*-factors of $R_1(F) = 0.0516$ and $wR_2(F^2) = 0.125$ were obtained. Details are listed in Tables 1–3.

The disorder of Ga was observed for several crystals. The amount of Ga on site 2*b* was between 14% and 16%. The data given above represent the results for the best refinement and were obtained from the single crystal used for the EDX and WDX measurements.

Cr_2GaC: A black hexagonal platelet was isolated from the Ga melt. All reflections were indexed with a hexagonal unit cell with lattice parameters of $a = 2.9008(4)$ Å and $c = 12.632(3)$ Å. The refinement was started with the parameters of a Cr_2AlC type [8] and performed quick convergence. Finally *R*-factors of $R_1(F) = 0.0174$ and $wR_2(F^2) = 0.0461$ were obtained with 90 unique reflections (63 with $I > 2\sigma(I)$) and nine parameters. Details are listed in Tables 1–3.

$V_2Ga_{1-x}Al_xC$ ($x \approx 0.43$ and 0.56): A black hexagonal platelet was isolated from the Ga/Al-melt. All reflections were indexed with a hexagonal unit cell. The lattice parameters were in good agreement with the powder data. For $V_2Ga_{0.57}Al_{0.43}C$ the values were $a = 2.925(1)$ Å and $c = 12.959(9)$ Å, for $V_2Ga_{0.44}Al_{0.56}C$ $a = 2.920(1)$ Å and $c = 13.029(8)$ Å. The refinement was started with the parameters of a Cr_2AlC-type [8] and performed quick convergence. The mixed occupation of site 2*d* by Ga and Al was obvious from difference Fourier syntheses. The ratio Ga:Al was refined as a free parameter. For $V_2Ga_{0.57}Al_{0.43}C$ the final *R*-factors were $R_1(F) = 0.0158$ and $wR_2(F^2) = 0.0357$ (113 unique reflections, 77 with $I > 2\sigma(I)$) and for $V_2Ga_{0.44}Al_{0.56}C$ $R_1(F) = 0.0278$ and $wR_2(F^2) = 0.0636$ (117 unique reflections, 75 with $I > 2\sigma(I)$). Details are listed in Tables 1–3.

$Cr_2Ga_{1-x}Al_xC$ ($x \approx 0.60$): A small fragment of a black hexagonal platelet was used for the structure analysis. All reflections were indexed with a hexagonal unit cell with lattice parameters of $a = 2.8752(17)$ Å and $c = 13.679(9)$ Å. According to the experimental conditions the refinement was started with the parameters of Cr_2GaC. Surprisingly the refinement presented different results. The site 2*a* which is usually occupied by C seemed to be empty, while the difference Fourier synthesis showed a residual electron density of 6.7 e$^-$/Å^3 at a site 4*e* with $z = 0.1552$, i.e. the octahedral voids between the Cr- and Ga-layers. The occupation of this site by carbon led to an occupation of 50%, *R*-values of $R_1 = 0.062$ and $wR_2(F^2) = 0.137$ and the expected/assumed composition Cr_2GaC. The refinement with a free occupation factor for Ga improved the *R*-values (0.051 and 0.112, respectively; sof(Ga) = 84%) but did not change the structure model, i.e. the site

Table 3
Selected distances (in (Å)) and angles (in (deg)), esd's in parentheses.

Ti_2GaC			
Ti–C	2.120 (1) 3*x*	Ga–Ga	3.0764 (4) 6*x*
Ti–Ga	2.8174 (14) 3*x*	Ga–Ti	2.8174 (14) 6*x*
Ti–Ti	2.918 (3) 3*x*	C–Ti	2.120 (1) 6*x*
Ti–Ti	3.0764 (4) 6*x*	Ti–C–Ti	86.97 (6)/93.03 (6)
Ti_4GaC_3			
Ti1–C1	2.123 (8) 3*x*	Ti2–C1	2.133 (8) 3*x*
Ti1–Ga	2.821 (1) 3*x*	Ti2–C2	2.203 (2) 3*x*
Ti1–Ti2	2.949 (3) 3*x*	Ti2–Ti1	2.949 (3) 3*x*
Ti1–Ti1	3.0690 (4) 6*x*	Ti2–Ti2	3.0690 (4) 6*x*
		Ti2–Ti2	3.160 (3) 3*x*
Ga–Ti1	2.821 (1) 6*x*	Ti2–C1–Ti2	87.7 (1)
Ga–Ga	3.0690 (4) 6*x*	Ti1–C1–Ti1	92.6 (5)
C1–Ti1	2.123 (8) 3*x*	Ti1–C1–Ti2	92.0 (5)/179.6 (1)
C1–Ti2	2.133 (8) 3*x*	Ti2–C2–Ti2	88.3 (1)
C2–Ti2	2.203 (2) 6*x*	Ti2–C2–Ti2	91.7 (1)
Cr_2GaC			
Cr–C	1.9913 (4) 3*x*	Ga–Ga	2.9008 (4) 6*x*
Cr–Ga	2.6710 (6) 3*x*	Ga–Cr	2.6710 (6) 6*x*
Cr–Cr	2.729 (1) 3*x*	C–Cr	1.9913 (4) 6*x*
Cr–Cr	2.9008 (4) 6*x*	Cr–C–Cr	86.50 (2)/93.50 (2)
$V_2Ga_{0.44}Al_{0.56}C$			
V–C	2.023 (1) 3*x*	Al/Ga–Al/Ga	2.920 (2) 6*x*
V–Al/Ga	2.724 (1) 3*x*	Al/Ga–V	2.724 (1) 6*x*
V–V	2.800 (2) 3*x*	C–V	2.023 (1) 6*x*
V–V	2.920 (2) 6*x*	V–C–V	87.59 (4)/92.41 (4)
$V_2Ga_{0.57}Al_{0.43}C$			
V–C	2.0225 (8) 3*x*	Al/Ga–Al/Ga	2.925 (1) 6*x*
V–Al/Ga	2.716 (1) 3*x*	Al/Ga–V	2.716 (1) 6*x*
V–V	2.794 (2) 3*x*	C–V	2.0225 (8) 6*x*
V–V	2.925 (1) 6*x*	V–C–V	87.37 (3)/92.63 (3)
$Cr_2Al_{0.60}Ga_{0.40}C$			
Cr–C	1.980 (1) 3*x*	Al/Ga–Al/Ga	2.875 (2) 6*x*
V–Al/Ga	2.669 (2) 3*x*	Al/Ga–Cr	2.667 (2) 6*x*
V–Cr	2.729 (1) 3*x*	C–Cr	1.980 (1) 6*x*
V–Cr	2.875 (2) 6*x*	Cr–C–Cr	86.88(2)/93.12(2)

2*a* remained empty and the site 4*f* half occupied. All in all the results seemed to be plausible. But the usual check of the composition by EDX had shown that these crystals contain considerable amounts of aluminium with a molar ratio for Cr:Al:Ga of 66:20:14. Therefore the structure model was modified when taking into account a mixed Ga/Al occupation of site 2*d*. Now the 2*a* site is fully occupied by carbon and the 4*e* site is empty. Furthermore the *R*-factors were significantly lower and the displacement parameters similar to those of Cr_2GaC. The ratio Al:Ga was found to be 59.9:40.1(4)% in excellent agreement with the EDX measurements. Finally *R*-factors of $R_1(F) = 0.032$ and $wR_2(F^2) = 0.086$ were obtained with 88 unique reflections (58 with $I > 2\sigma(I)$) and nine parameters. Details are listed in Tables 1–3. A note, the observations described above were made for several crystals.

Further details on the structure refinements (complete list of distances and angles, F_o/F_c-list) may be obtained from: Fachinformationszentrum Karlsruhe, D-76344 Eggenstein-Leopoldshafen (Germany) (fax: +49 724 808 666; e-mail: crysdata@fiz-karlsruhe.de) on quoting the registry numbers CSD—419117 (Ti_2GaC), 419118 (Ti_4GaC_3), 419116 (Cr_2GaC), 419245 ($V_2Ga_{0.44}Al_{0.56}C$), 419246 ($Cr_2Ga_{0.57}Al_{0.43}C$), and 419119 ($Cr_2Ga_{0.4}Al_{0.6}C$).

3. Results and discussion

The investigations of the system Ti/Ga/C indicate that temperature plays a key role in the syntheses using the auxiliary metal technique. Fig. 1 shows the powder diagrams recorded from samples obtained at different temperatures. At 1680 °C only the reflections of TiC were observed. At 1600 °C the main product remains as TiC but the reflection profiles show a broadening probably caused by the formation of non-stoichiometrical TiC_{1-x}. At 1500 °C, it is clear a ternary carbide forms. The diagram shows a mixture of Ti_2GaC and TiC. At 1300 °C, the main products are Ti_4GaC_3 and Ti_2GaC while TiC is not observed.

The results confirm the general tendency that at higher temperatures the formation of simple compounds (binary carbide) is favoured. At lower temperatures the more complex ternary carbides Ti_2GaC and/or Ti_4GaC_3 are formed. Similar observations were made for other ternary carbides synthesised by the auxiliary metal technique [20,21].

Ti_2GaC: The crystal structure of Ti_2GaC (Fig. 3) belongs to the Cr_2AlC type, a so-called 211- or H-phase, confirming the results of Jeitschko et al. [9e] ($a = 3.064$ Å, $c = 13.305$ Å). The metal atoms form a hexagonal closest packing (hcp) with Ga in every third layer. The C atoms occupy all octahedral voids between the layers of Ti atoms. Because the 211-phase bases on a hcp, both metals have an anticuboctahedral coordination. For Ga it is built up by six Ga and six Ti atoms, for Ti three Ga and nine Ti atoms with three additional C atoms.

Distances are determined by the lattice constants and the free site parameter z_{Ti}. With a value of 0.0865 it is quite close to that originally found for Cr_2AlC by Jeitschko et al. [8] and recently confirmed for V_2AlC [12]. The small deviation from the ideal value for a hcp ($z_{Ti} = 1/12 \approx 0.0833$) can be explained by the influence of the occupation of the octahedral site by carbon. The Ti–C distances of 2.120 Å are slightly shorter than in the binary TiC (2.164 Å) and the CTi_6 octahedra are compressed along [001]

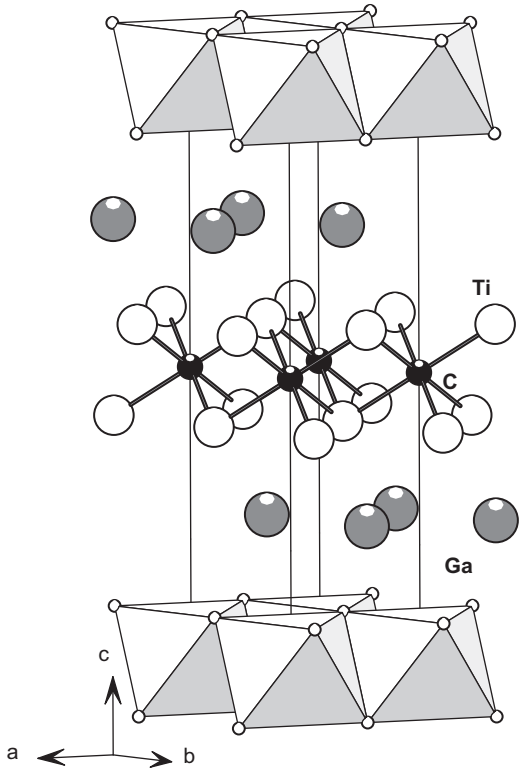

Fig. 3. Crystal structure of Ti_2GaC.

(Ti–C–Ti: 93.0°). This is a well-known phenomenon in 211-phases. The shortest metal–metal distances are between Ga and Ti layers (2.817 Å), and the longest within the layers (3.076 Å, i.e. lattice parameter *a*).

Ti_4GaC_3: Ti_4GaC_3 represents the forth example for a 413-phase. Its crystal structure (Fig. 4) consists of a closest packing of metal atoms with a layer sequence *b*A*c*B**A**B*c*A*b*C*a*B**C**B*a*C*b* and carbon atoms in octahedral voids (Ga layers in bold letters, C in octahedral voids and italics). The coordination polyhedra of the atoms (Fig. 5) can be derived directly from this building principle, i.e. an anticuboctahedron (six Ga and six Ti atoms) for gallium, a cuboctahedron (12 Ti-atoms) plus six C-atoms for Ti2, an anticuboctahedron (nine Ti and three Ga atoms) plus three C atoms for Ti1 and Ti_6 octahedra for both of the C atoms.

According to the intergrowth concept the carbide part is enlarged compared to Ti_2GaC and now contains three layers of the NaCl type. There are two different C-atoms with C2 in the "central" layer and C1 in the "outer" layer. These differences are also mirrored in the Ti–C distances. The "central" distance C2–Ti2 amounts to 2.203 Å and is slightly longer than in binary TiC. The "outer" distance C1–Ti1 is significantly shorter (2.120 Å) with C1–Ti2 in between (2.133 Å). Similar observations were made for Ta_4AlC_3 (2.230/2.206/2.166 Å; TaC: 2.228 Å). To emphasise, for Ti_2GaC the CTi_6 octahedra are compressed along [001]. According to the position of Ti_4GaC_3 between Ti_2GaC and TiC this compression is also present in the "outer"octahedron (Ti1–C1–Ti1: 92.8°; Ti2–C1–Ti2: 91.7°). In contrast the "central" octahedron is slightly elongated (Ti2–C2–Ti2: 88.3°) and accordingly the Ti2–Ti2 distances between the central layers are longer (3.160 Å) than in TiC (3.06 Å) while the outer distances Ti1–Ti2 are shorter (2.949 Å).

The intermediate position of Ti_4GaC_3 between TiC and Ti_2GaC is also valid for the valence sums calculated according to Brown [22]. Although the concept of valence sums is more adequate for ionic and covalent compounds, it is also applicable for intermetallics to get qualitative statements. For TiC the values are 7.10 for Ti and 4.16 for C. In Ti_2GaC the valence sums are significantly lower for Ti (5.79, 2.34 from Ti–C bonds) because there are only three Ti–C bonds, and higher for C (4.69). Ga has a value of 2.61. In Ti_4GaC_3 the values for Ti2 (7.12, 4.14 from Ti–C bonds) and C2 (3.74) are very close to TiC while those for Ti1 (5.70, 2.32 from Ti–C bonds), C1 (4.59) and Ga (2.61) are similar to Ti_2GaC. Therefore, an estimation of bond distances and atomic coordinates for MAX-phases based on valence sums and the general building principle described in [11] is possible [23].

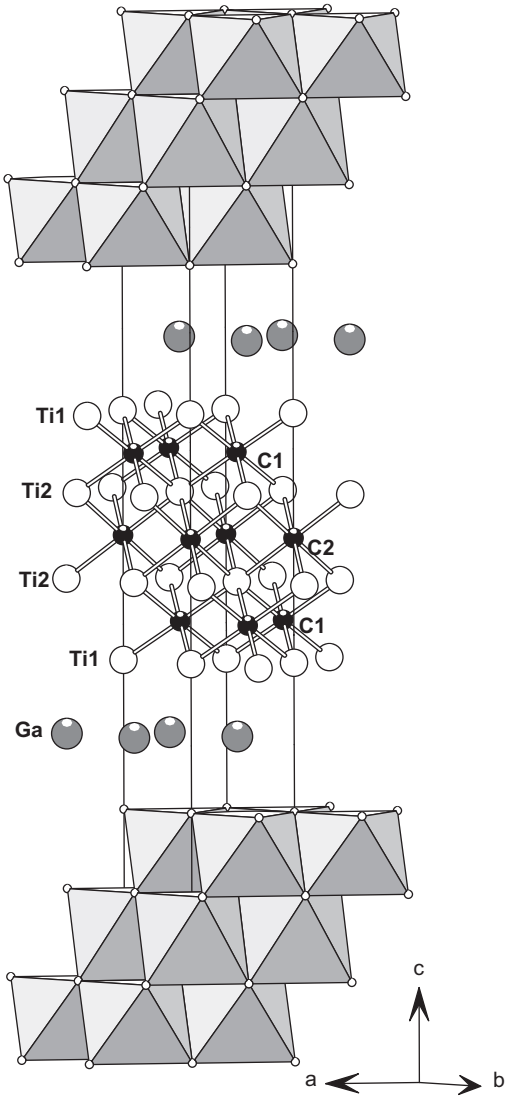

Fig. 4. Crystal structure of Ti_4GaC_3.

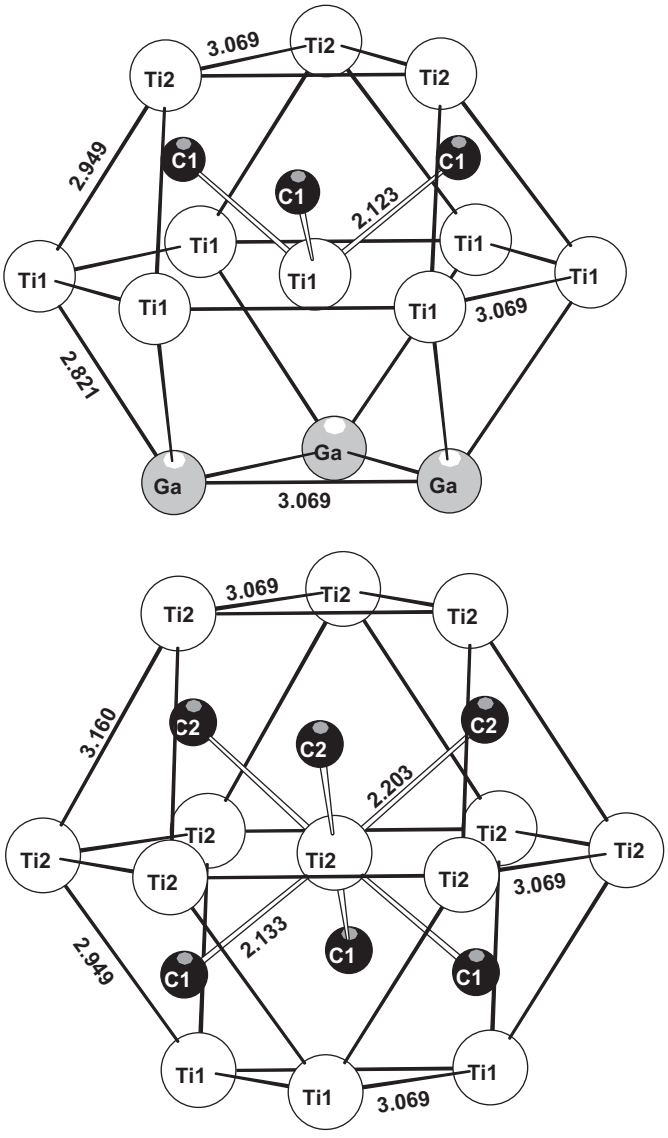

Fig. 5. Coordination polyhedra of Ti in Ti_4GaC_3.

The occupation of site 2*b* (instead of site 2*c*) by Ga changes the stacking sequence from $(hhhcc)_2$ to $(hcccc)_2$. The coordination of the 2*b*-site is still an anticuboctahedron but the surrounding of Ti1 is changed to a cuboctahedron. The splitting of the Ga-site was not limited to a singular crystal but was also confirmed for several other crystals from different batches. Values between 12% and 14% were found for the occupation of site 2*b*. A similar disorder of the metal layer was also observed for the MAX-phase Ti_3AlC_2 [20,23]. Two polymorphs are described for Ti_3SiC_2 [24]. The difference between both is the position of Si on one of these two sites. For Ti_3GeC_2 there is a pressure-induced phase transition at 27 GPa between these two polymorphs [25].

Very recently Lin et al. reported on a second modification of Ta_4AlC_3 [26]. On the basis of TEM/STEM investigations and electron diffraction (SAED, CBED) they described a structure where all metal atoms were in a hexagonal closest packing. This would imply that the CTa_6-octahedra share common faces along [001]. Although many binary and ternary transition metal carbides with CTM_6 octahedra are known [1,7] there is no example with this structural feature. One explanation would be the formation of vacancies as proven for $V_{12}Al_3C_8$ [12], but also in this case there are only cubic sequences within the carbide layers.

Cr_2GaC: Cr_2GaC also belongs to the Cr_2AlC-type, and confirms the earlier report of Jeitschko et al. [9a]. Based on powder data, they assigned it to an H-phase with lattice constants of $a = 2.886$ Å and $c = 12.616$ Å. The differences between Cr_2GaC and Ti_2GaC are very small. Because of the smaller metal radius of Cr (Cr: 1.28 Å, Ti: 1.45 Å) lattice constants and distances are slightly reduced. The free site parameter z_{Cr} is nearly the same (0.0853). The Cr–C-distances of 1.991 Å are slightly shorter than in the metastable binary CrC (2.02 Å) [27]. The CCr_6-octahedra are compressed in the crystallographic *z*-direction leading to a Cr–C–Cr angle of 93.5° and Cr–Cr distances of 2.729 Å between the Cr-layers. The shortest metal–metal distances are between Ga- and Cr-layers (2.671 Å), the longest ones within the layers (2.901 Å).

$V_2Ga_{1-x}Al_xC$ and $Cr_2Ga_{1-x}Al_xC$: The values of the lattice parameters obtained both from powders and single crystals are consistent with the formation of an ideal solid solution and follow Vegard's law. A special feature of these solid solutions is that the electron density on the Ga/Al site is very similar to vanadium and chromium, respectively. As a consequence all strong reflections can be indexed by a subcell with $c' = 1/3c$ compatible with a simple hexagonal closest packing. The super cell is only defined by the carbon atoms. In the powder patterns the strongest super cell reflections 002 and 104 have only 1% intensity of the strongest reflection 103. Therefore reliable statements on the localisation of the carbon atoms require the investigation of single crystals.

The example of $V_2Ga_{1-x}Al_xC$ shows that even the *z*-parameter of V follows Vegard's law. For V_2AlC z_V is 0.08558 [12]. Because this is the only free site parameter of a 211-phase lattice parameters and all distances of solid solutions can be derived from the corresponding ternary compounds.

The results on the refinement of the solid solutions were included to this publication for several reasons. First it proofs the existence of the solid solutions $V_2Ga_{1-x}Al_xC$ and $Cr_2Ga_{1-x}Al_xC$. The ratio of the metals can reliably be determined on the basis of single crystal X-ray data in these cases. Solid solutions are very common in MAX-phases and can occur for different positions, i.e. $Ti_{2-x}V_xAlC$ [28], $Ti_3Al_{1-x}Si_xC_2$ [23], $Ti_2Sn_{1-x}Al_xC$ [29], $Ti_3Sn_{1-x}Al_xC_2$ [23], $Ti_2AlC_{1-x}N_x$ [30], $Ti_4Al_{1-x}Sn_xN_{1-y}C_y$ [13]. These solid solutions are of practical importance because they strongly influence the material properties [30]. Second it is an example for the easy occurrence of unexpected contaminations, especially in those cases where the sample is not completely characterised, i.e. single crystals by X-ray investigations or electron microscopy. Third we have learned that the refinement may converge to a local minimum with a plausible structure which may not be the right solution. This may be caused by the high (pseudo)symmetry of MAX-phases and the great difference of the electron numbers (i.e. Ta/Sn and C/N), in combination with stacking faults and different types of solid solutions. An example for possible problems is the confusion on the structure of Ti_4AlN_3 [31].

4. Conclusions

The use of molten metals as a solvent enables the synthesis of new MAX-phases and the growth of single crystals. The access to reliable structural data on the basis of single crystals allows a more detailed discussion of geometrical relations in 413-phases. Usually atomic parameters are derived from a comparison of calculated and observed intensities. While an estimation of the metal parameters is obtainable from powder intensity data the reliable determination of the carbon sites is only possible from single crystal and/or neutron diffraction measurements [32].

The building principle of MAX-phases $(MC)_nMA$ is quite simple. They are intermediates between an alloy *MA* with hexagonal closest packing and the binary carbide *MC* with NaCl structure, where *n* determines the cut-out of the carbide part. In general the structural details follow this connection. For higher numbers of *n* the *M*–C distances approach those of the binary carbide while the most significant deviations are observed for the carbide layer closest to the layer of *A*.

Despite the close relations between the different MAX-phases there are some systematic differences. For the Al-containing MAX-phases the lattice parameter *a* is slightly larger for the 413-phases (Ti_4AlN_3 [4], Ta_4AlC_3 [11] and V_4AlC_{3-x} (or $V_{12}Al_3C_8$, respectively) [12]) than for the corresponding 211-phases. The same is true for the 312-phases Ta_3AlC_2 [11] and Ti_3AlC_2 [20,33]. The opposite behaviour is observed for Ti_4GaC_3 and Ti_2GaC. With $A = Ge$, the only example where two different MAX-phases are described, the *a* lattice parameters are virtually identical (Ti_3GeC_2: $a = 3.077$ Å [34], Ti_2GeC: $a = 3.079$ Å [9b]). Obviously the atomic radius of the metal *A* has a subtle influence on the *M*–C interaction which is planned to be investigated by band structure calculations [35]. This more complex behaviour is found for the 211-phases, too. Although the atomic radius of Ga is smaller than for Al, the lattice parameter *a* of the Ga-containing H-phases is larger than for the corresponding Al-phases (see Table 4). But in total the unit cell volume of the Ga-phases is smaller. A more detailed discussion of the geometrical aspects of 211-phases will follow based on future single crystal data for single crystals obtained through the auxiliary metal technique. This is in line with our previous results on the synthetic potential of metallic melts [36], which enables the formation of new high-melting compounds at lower temperatures and/or the growth of single crystals [37].

For the 413-phase Ti_4GaC_3, it was demonstrated that a disorder of Ga occurs systematically. Similar stacking variants/faults were already reported for other MAX-phases, mainly on the basis of (HR)TEM investigations [38].

The mechanical properties of MAX-phases are intensely investigated (for example [2,5]). According to the lack of single crystals of sufficient size hardness measurements are done on sintered samples. Additionally the compressibility was measured [39] in order to estimate the hardness. The only exception seems to be Ti_3SiC_2 [40] where single crystals are grown via a CVD-process. The access to well-shaped single crystals (Fig. 2) via metallic melts enables (micro)hardness measurements of further MAX-phases. The corresponding measurements are in progress [41].

Table 4
Lattice parameters (in (Å)) and metal radii (in (Å), according to [43]) of H-phases M_2AC (M = Ti, V, Cr, Nb, Ta, Mo; A = Al, Ga); powder data.

Compound	a	c	V	r(TM)	r(M')	Reference
Ti_2GaC	3.066	13.312	108.37	1.45	1.39	This work
Ti_2AlC	3.056	13.623	110.18	1.45	1.43	[42]
V_2GaC	2.938	12.84	95.98	1.36	1.39	[8]
V_2AlC	2.916	13.130	96.69	1.36	1.43	[12]
$V_2Ga_{0.44}Al_{0.56}C$	2.921	13.047	96.41	1.36	1.39/1.43	This work
$V_2Ga_{0.57}Al_{0.43}C$	2.928	12.998	96.51	1.36	1.39/1.43	This work
Cr_2GaC	2.893	12.665	91.65	1.28	1.39	This work
Cr_2AlC	2.860	12.82	90.81	1.28	1.43	[8]
$Cr_2Ga_{0\ 4}Al_{0\ 6}C$	2.875	12.679	90.77	1.47	1.39/1.43	This work
Nb_2GaC	3.131	13.565	115.16	1.47	1.39	[9d]
Nb_2AlC	3.103	13.83	115.32	1.47	1.43	[8]
Ta_2GaC	3.104	13.57	113.23	1.46	1.39	[9e]
Ta_2AlC	3.075	13.83	113.25	1.46	1.43	[8]
Mo_2GaC	3.017	13.18	103.90	1.40	1.39	[8]

MAX-phases have a strong tendency to form solid solutions which may be important for applications. Vegard's law is valid for all structural parameters. The example of the solid solution $V_2Ga_{1-x}Al_xC$ shows that the value of x can be triggered by the ratio Ga:Al of the melt.

Acknowledgments

Thanks are due to Bayerisches Geo-Institut (BGI, Universität Bayreuth) for the access to WDX measurements and to Detlev Krauße for his support. M.K. thanks the OBW (Ontario-Baden Württemberg) exchange program for support.

References

[1] [a] R. Freer (Ed.), The Physics and Chemistry of Carbides, Nitrides and Borides, Kluwer Academic Publishers, Dordrecht, 1990;
[b] P. Ettmayer, W. Lengauer, in: Encyclopedia of Inorganic Chemistry, Wiley, Chichester, England, 1996, pp. 519–531;
[c] L.E. Toth, in: Transition Metal Carbides and Nitrides, Academic Press, New York, 1971;
[d] H. Nowotny, Angew. Chem. 84 (1972) 973;
H. Nowotny, Angew. Chem. Int. Ed. Engl. 11 (1972) 906.
[2] [a] M.W. Barsoum, T.J. El-Raghi, Am. Ceram. Soc. 79 (1996) 1953;
[b] M.W. Barsoum, T. El-Raghi, Am. Sci. 89 (2001) 334.
[3] N.V. Tzenov, M.W. Barsoum, J. Am. Ceram. Soc. 83 (2000) 825.
[4] C.J. Rawn, M.W. Barsoum, T. El-Raghi, A.T. Procopio, C.M. Hoffmann, C.R. Hubbard, Mater. Res. Bull. 35 (2000) 1785.
[5] M.W. Barsoum, Progr. Solid State Chem. 28 (2000) 201.
[6] M.W. Barsoum, M. Radovic, T. Zhen, P. Finkel, S.R. Kalidindi, Phys. Rev. Lett. 94 (2005) 085501.
[7] P. Villars, L.D. Calvert, Pearson's Handbook, Crystallographic Data for Intermetallic Phases, ASM International, Materials Park, OH, 1997.
[8] W. Jeitschko, H. Nowotny, Monatsh. Chem. 94 (1963) 672.
[9] [a] W. Jeitschko, H. Nowotny, F. Beneshovsky, Monatsh. Chem. 94 (1963) 844;
[b] W. Jeitschko, H. Nowotny, F. Beneshovsky, Monatsh. Chem. 94 (1963) 1198;
[c] W. Jeitschko, H. Nowotny, F. Beneshovsky, Monatsh. Chem. 95 (1964) 156;
[d] W. Jeitschko, H. Nowotny, F. Beneshovsky, Monatsh. Chem. 95 (1964) 178;
[e] W. Jeitschko, H. Nowotny, F. Beneshovsky, Monatsh. Chem. 95 (1964) 431.
[10] [a] X.H. Wang, Y.C. Zhou, Acta Mater. 50 (2002) 3141;
[b] X.H. Wang, Y.C. Zhou, Oxide Met. 59 (2003) 303;
[c] O. Wilhelmsson, J.-P. Palmquist, E. Lewin, J. Emmerlich, P. Eklund, P. Persson, H. Högberg, S. Li, R. Ahuja, O. Ericsson, L. Hultman, U. Jansson, J. Cryst. Growth 291 (2006) 290;
[d] H. Högberg, L. Hultman, J. Emmerlich, T. Joelsson, P. Eklund, J.M. Molina-Aldareguia, J.-P. Palmquist, O. Wilhelmsson, U. Jansson, Surf. Coat. Technol. 193 (2005) 6.
[11] J. Etzkorn, M. Ade, H. Hillebrecht, Inorg. Chem. 46 (2007) 1410.
[12] J. Etzkorn, M. Ade, H. Hillebrecht, Inorg. Chem. 46 (2007) 7646.
[13] H. Lückeroth, Diploma Thesis, University of Bonn, Germany, 1998.
[14] F. Eggert, Microchim. Acta 155 (2006) 129.
[15] [a] G.F. Bastin, H.J.M. Heijligers, Microbeam Anal. 1 (1993) 61;
[b] G.F. Bastin, H.J.M. Heijligers, J. Solid State Chem. 154 (2000) 177.
[16] Because the structure of Cr_7C_3 was derived from powder data [17] F. McClune, Powder Diffr. 1 (1986) 77; [b] R. Fruchart, A. Rouault, Ann. Chim. (Paris) 4 (1969) 143] we refined the structure from single crystal data which confirmed the proposed structure. Mn_7C_3 type, $oP40$, $a = 4.5285(13)$ Å, $b = 7.0158(7)$ Å, $c = 12.1379(13)$ Å, 601 refl., 53 param., $R_1(F) = 0.0412$, $wR_2(F^2) = 0.1115$. Further detailed are available on CSD–419120.
[17] [a] F. McClune, Powder Diffr. 1 (1986) 77;
[b] R. Fruchart, A. Rouault, Ann. Chim. (Paris) 4 (1969) 143.
[18] Programme XSHAPE/XRED, STOE Cie, Darmstadt, Germany, 2003.
[19] G.M. Sheldrick, Programme SHELXL, University of Göttingen, Germany, 1997.
[20] M. Ade, Ph.D. Thesis, University of Freiburg, Germany, 1997.
[21] J. Etzkorn, Ph.D. Thesis, University of Bayreuth, Germany, 2002.
[22] I.D. Brown, J. Appl. Cryst. 29 (1996) 479.
[23] M. Kleczek, D. Kotzott, J. Etzkorn, M. Ade, H. Hillebrecht, J. Am. Ceram. Soc., to be submitted.
[24] [a] L. Farber, I. Levin, M.W. Barsoum, T. El-Raghy, T. Tzenov, J. Appl. Phys. 86 (1999) 2540;
[b] R. Yu, Q. Zhan, L.L. He, Y.C. Zhou, H.Q. Ye, J. Mater. Res. 17 (2002) 948.
[25] Z. Wang, C.S. Zha, M.W. Barsoum, Appl. Phys. Lett. 85 (2004) 3453.
[26] [a] Z.J. Lin, M.J. Zhuo, Y.C. Zhou, M.S. Li, J.Y. Wang, J. Mater. Res. 21 (2006) 2587;
[b] Z.J. Lin, M.J. Zhuo, Y.C. Zhou, M.S. Li, J.Y. Wang, J. Mater. Res. 22 (2007) 816.
[27] [b] E. Bouzy, E. Bauer, G. LeCaer Grosse, Phil. Mag. B 68 (1993) 619.
[28] H. Nowotny, P. Rogl, J.C. Schuster, J. Solid State Chem. 44 (1982) 126.
[29] J. Etzkorn, M. Kleczek, D. Kotzott, M. Ade, H. Hillebrecht, unpublished results.
[30] M.W. Barsoum, M. Ali, T. El-Raghy, Metal. Mater. Trans. A 31 (2000) 1857.
[31] [b] M.W. Barsoum, J.C. Schuster, J. Am. Ceram. Soc. 81 (1998) 785;
[c] H.D. Lee, W.T. Petruskey, J. Am. Ceram. Soc. 81 (1998) 787;
[d] M.W. Barsoum, L. Farber, I. Levin, A. Procopio, T. El-Raghy, A. Berner, J. Am. Ceram. Soc. 82 (1999) 2545.
[32] C.J. Rawn, E.A. Rayzaut, C.R. Hubbard, M.W. Barsoum, T. El-Raghy, Mater. Sci. Forum 321/324 (2000) 889.
[33] E. Wu, J. Wang, H. Zhang, Y. Zhou, K. Sun, Y. Xue, Mater. Lett. 59 (2005) 2715–2719.
[34] H. Wolfsgruber, H. Nowotny, F. Beneshovsky, Monatsh. Chem. 98 (1967) 2403.
[35] M. Schroeder, H. Hillebrecht, unpublished results.
[36] [a] P. Lebeau, C. R. Acad. Sci. (Paris) 27 (1898) 393;
[b] H. Scheel, D. Elwell, Crystal Growth from High-Temperature Solutions, Academic Press, London, 1975;
[c] M.G. Kanatzidis, R. Pöttgen, W. Jeitschko, Angew. Chem. 117 (2005) 7156;
M.G. Kanatzidis, R. Pöttgen, W. Jeitschko, Angew. Chem. Int. Ed. 44 (2005) 6996.
[37] [a] H. Hillebrecht, K. Gebhardt, Z. Kristallogr. Suppl. 18 (2001) 155;
[b] H. Hillebrecht, M. Ade, Angew. Chem. 110 (1998) 981;
H. Hillebrecht, M. Ade, Angew. Chem. Int. Ed. 37 (1998) 935;
[c] H. Hillebrecht, K. Gebhardt, Angew. Chem. 110 (2001) 1492;
H. Hillebrecht, K. Gebhardt, Angew. Chem. Int. Ed. 40 (2001) 1445;
[d] F. Meyer, H. Hillebrecht, J. Alloys Compd. 252 (1997) 98;
[e] H. Hillebrecht, F. Meyer, Angew. Chem. 108 (1996) 2655;
H. Hillebrecht, F. Meyer, Angew. Chem. Int. Ed. 35 (1996) 2499.
[38] Z. Lin, M. Li, Y. Zhou, J. Mater. Sci. Technol. 23 (2007) 145.
[39] [a] Z. Wang, C.S. Zha, M.W. Barsoum, Appl. Phys. Lett. 85 (2004) 3453;
[b] B. Manoun, R.P. Gulve, S.K. Saxena, S. Gupta, M.W. Barsoum, C.S. Zha, Phys. Rev. B 73 (2006) 024110;
[c] B. Manoun, S.K. Saxena, T. El-Raghi, M.W. Barsoum, Appl. Phys. Lett. 88 (2006) 201902.
[40] J.J. Nickl, K.K. Schweitzer, P. Luxenberg, J. Less-Common Met. 26 (1972) 335.
[41] D. Kotzott, H. Hillebrecht, unpublished results.
[42] S. Sridharan, H. Nowotny, S.F. Wayne, Monatsh. Chem. 114 (1983) 127.
[43] K. Schubert, Kristallstrukturen Zweikomponentiger Phasen, Springer, Berlin, 1964.